Global NEST Journal, Vol 26, No 5, 05650

Composite electrospun membranes based on PET-PAN modified with LDH-hybrid as promising adsorbent for pollutants removal from wastewater

Abdul Majeed Pirzada[1]*, Imran Ali[1]*, Nabi Bakhsh Mallah[2] and Ghulamullah Maitlo[3]

[1]Department of Environmental Sciences, Sindh Madressatul Islam University, Aiwan e Tijarat Road Karachi 74000, Pakistan

[2]Faculty of Engineering, Science and Technology, Hamdard University, Shahra e Madinat-ul-Hikmat, Karachi 74600, Pakistan

[3]Department of Chemical Engineering, Dawood University of Engineering & Technology, New M. A Jinnah Road, Karachi 74800, Pakistan

Received: 08/12/2023, Accepted: 11/05/2024, Available online: 16/05/2024

*to whom all correspondence should be addressed: e-mail: ampirzada@smiu.edu.pk, imran.ali@smiu.edu.pk

https://doi.org/10.30955/gnj.005650

Graphical abstract

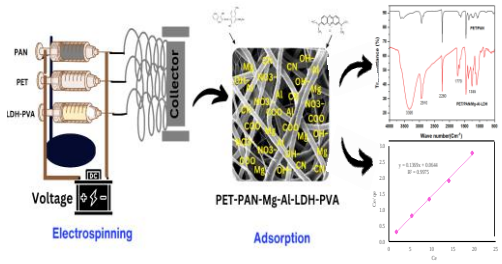

Abstract

The current work reveals the fabrication of a novel nanofiber composite membrane of PET-PAN modified with Mg-Al-LDH-PVA through electrospinning process. The nanocomposite membranes characterization was conducted with different techniques i.e. SEM, EDS, FTIR, XRD, and water contact angle to evaluate the structure and surface morphology. The optimized nanomembrane was utilized as a useful adsorbent for removal of toxic anionic dye Eriochrome Black T (EBT) and cationic dye Methylene blue (MB) from wastewater. Experimental results identified that $PPLP_3$ membrane has a potential for the removal of EBT (83%) and MB (52%) at pH 3 and 7, respectively, from aqueous solution. The optimum adsorption capacity of $PPLP_3$ nanocomposite membrane was identified and calculated as 7.3 $mg.g^{-1}$ followed by the pseudo 2nd order kinetics and Langmuir adsorption isotherm fit well with R^2 values of 0.964 and 0.997, respectively. The synthesized nanocomposite membrane could be utilized for effective adsorption of contaminations from different wastewaters.

Keywords

Electrospun membranes; Nanocomposite polymers; Layered double hydroxides; adsorption; dye pollutants.

1. Introduction

Water is regarded as the most important natural resource that is found on this planet. For the survival of any living thing, water is the most required thing. Owing to having a high level of solubility, water is regarded as the universal solvent (Ahmad *et al*. 2015; Zhang *et al*. 2016). The key environmental challenge experienced by the people of the world is to maintain the quality of water. As the current level of available reserves of fresh water is insufficient and getting more and more polluted by the passage of time. Such water reserve depletion is causing an inability due to the excess consumption by the increased level of population growth, urbanization, industrialization, agricultural and other activities (Ayandiran *et al.* 2018; da Silva Alves *et al.* 2021; Jeong *et al*. 2019).

Water contamination is regarded as serious problem worldwide, which has significantly affected the health of people and the life present in the ecosystem (Anandh Babu *et al.* 2023; Preethi & Jeyanthi 2023). Polluted water becomes the main cause of various diseases in the human being which also posed challenges in the field of sciences (Picón *et al.* 2022). The various industries such as cosmetics, plastics, food, textiles, rubber, paper, and printing have released a very large quantity of wastewater which contains the significant amount of toxic indispensable dyes (Khalid *et al.* 2018; Radoor *et al.* 2020). The untreated wastewater discharge of these dyes into the water bodies give serious threats to aquatic life and human being (Manzar *et al.* 2019). Therefore, introducing new effective methods and materials for removing the pollutants and dyes from wastewater is drastically required (Akram *et al*. 2023; Bano *et al*. 2024; Inam *et al*. 2021; Kishore *et al*. 2023).

At present, the methods for treating dye wastewater comprise of different categories which include chemical, physical and biological processes. These methods contain several disadvantages, for example they take the high amount of energy along with higher level of costs and

produce highly toxic and hazardous byproducts. Therefore, the process of adsorption is regarded as one of the most promising approach because it is easy to operate, less costly and can be recycled with ease and efficient one in comparison with the other conventional techniques (Cheng *et al*. 2020; Z.-P. Hu *et al.* 2018).

Electrospinning nanofiber membranes are considered for having capability of dealing with the industrial wastewater, because their structure is highly adjustable along with higher efficiency, porosity, and higher surface area. These attractive characteristics make adsorbents to be prepared using the electrospinning membranes (Dai *et al.* 2018; Farooqi *et al.* 2021; Zhao *et al*. 2017; Zhu *et al.* 2021). At present, many studies are bringing the usage of different homopolymers such as polyethylene terephthalate (PET) and polyacrylonitrile (PAN). In order to prepare the composite membrane modified with the nanoparticles such as layer double hydroxides (LDH) and hybrids of polyvinyl alcohol (PVA) with the purpose of increasing the adsorption removal efficiency for pollutants (Ebrahimi *et al.* 2022; Khorram *et al.* 2017; Mittal 2021; Sajid *et al.* 2022).

Previously, many researchers have used different types of polymer combination for fabricating the electrospun nanofibers membrane in order to treat the wastewater. For example, synthesis of different LDHs including MgAl, NiFe and CoAl through co-precipitation technique for the elimination of Eriochrome Black T (EBT) dye and shows adsorption of 540.91 $mg.g^{-1}$, 132.49 $mg.g^{-1}$ and 419.87 $mg.g^{-1}$, respectively (Zubair *et al*. 2017). PVA-Starch modified ZSM-5 zeolite nanomembrane displayed an adsorption for EBT about 2.17 $mg.g^{-1}$ (Radoor *et al*. 2020). The layered Ag/PDA/PS nanomembrane was fabricated and showed a complete removal of EBT pollutant from effluent (Baig *et al*. 2022).

The study worked on the fabrication of Fe-SCD-Mg-Al-LDH through ion exchange reaction process and by the method of co precipitation to prepare composite and it display the capability of about 83.40 $mg.g^{-1}$ for color pollutant methylene blue (MB) adsorption (W. Hu *et al.* 2016). PVA-CS modified with nanoparticles $CeAlO_3$ showed the adsorption for MB about 817.81 $mg.g^{-1}$ (Shahverdi *et al.* 2022). The nanocomposite was fabricated with the help of LDH and activated carbon (AC) through the hydrothermal process. The prepared nanofiber mat showed exceptional attraction for the MB dyes and displayed 250.2 $mg.g^{-1}$ at PH 9. The prepared nanocomposite membrane shown higher efficiency at the room temperature about 816.0 $mg.g^{-1}$ (Aldawsari *et al*. 2021). PET NF-MWCNTs were prepared and estimated the adsorption for MB about 7.047 $mg.g^{-1}$ (Essa *et al*. 2022).

Therefore, in this study a new efficient PET-PAN modified using Mg-Al-LDH-PVA was synthesized with electrospun methodology for the removal of EBT and MB color pollutants from effluent. The objective of this research is the utilization of the developed novel membrane as an adsorbent material for the removal of the cationic and anionic dyes i.e. MB and EBT from the effluent. The effect of different operating parameters i.e., pH of solution, adsorption time, pollutant concentration, and membrane dosage were also checked. Adsorption isotherm and kinetics were performed to check the membrane efficiency. The comparison of the current study with other related studies were also performed. Additionally, the proposed adsorption mechanism for pollutant removal was suggested.

2. Methodology

2.1. Chemicals and materials

In this research, post-consumer waste bottles of PET were used. Likewise, other polymers and chemicals were used in this study, i.e. PVA with an average molecular weight (Mw) of 9,000–10,000 (80% hydrolyzed), white powder form PAN with Mw of 150,000, ($Mg(NO_3)_2.6H_2O$) magnesium nitrate hexahydrate of 99%), ($Al(NO_3)_3.9H_2O$) aluminum nitrate nonahydrate ≥ 98%), sodium carbonate powder (Na_2CO_3 ≥ 99.5%), hydrochloric acid (HCl, 37%), sodium hydroxide pellets (NaOH), and sulfuric acid (H_2SO_4), were received from Sigma-Aldrich, Burlington, USA. Also, various other solvents and dyes namely, N, N-Dimethyl formamide (DMF), trifluoro acetic acid (TFA), dichloro methane (DCM), EBT dye, and MB dye were got from Dae-Jung, Busan, South Korea. In addition, the distilled water and analytical research grade type of chemicals were utilized for the research experiments.

2.2. Fabrication of nanoparticles (LDH)

Nanoparticles (Mg-A1-LDH) were synthesized using the coprecipitation method (Alnaqbi *et al.* 2020; Qin *et al*. 2012). During nanoparticle synthesis, as precursors $Al(NO_3)_3.9H_2O$ and $Mg(NO_3)_2.6H_2O$ were used in a proportion of 1:3 (Mg:Al) and under constant pH conditions. 0.025 M of $Al(NO_3)_3.9H_2O$ and 0.075 M of $Mg(NO_3)_2.6H_2O$ of 50 mL mixed aqueous solution and then was added with 50 mL of 0.05 M of Na_2CO_3 and 1 M of NaOH with vigorous and continuous stirring (hotplate magnetic stirrer MS-H280-Pro, OniLab, CA USA). NaOH of 1 M solution was utilized to maintain the solution pH in 9.0-9.5 range. The slurry was aged for 12 h at the set temperature of 65°C. The obtained solid was then processed for centrifuge (80-2 Electronic centrifuge, Atlas medical italiano, China) and cleaned with deionized water several times and kept for drying for 12 h period in an oven (DHG-9202, SANFA, China) at a fixed temperature of 70°C.

2.3. Preparation of electrospinning polymer solution

Polymer solution of PET was prepared by cutting the post-consumer waste PET bottles into square shaped pieces of size $1x1cm^2$ followed by the cleaning and rinsing with deionized water for the electrospinning process. The PET bottle's pieces were then heated in ethanol solution for a duration of 30 min at 40°C to remove the contamination. 5 wt.% homogeneous solution was prepared by dissolving the PET bottle pieces in a DCM-TFA mixture having a ratio of 3:1, followed by mixing at duration of 4 h at room temperature using magnetic stirrer.

Similarly, PAN (8 wt.%) solution in DMF was prepared with continuous stirring for 12 h at ambient temperature. PVA

(8 wt.%) solution was prepared in distilled (double) water with continuous stirring for a duration of 5 h at 80°C. Mg-Al-LDH nanoparticles were mixed in PVA (10 gm) solution at different loadings (0.8, 1.2, and 1.6%) for making the Mg-Al-LDH-hybrid solution for $PPLP_1$, $PPLP_2$, and $PPLP_3$ membranes, respectively. Later, the resulting spinnable solution was homogenized by sonicating (Ultrasonic cleaner 2L, China) for 1 h at ambient temperature.

2.4. Fabrication of PET-PAN-LDH-Hybrid membrane

As reported in our previous study, PP and PPLP nanocomposite membranes were synthesized by using electrospinning technique (Pirzada *et al.* 2023). The ready electrospun polymer solutions were transferred into syringes of 10 mL capacity with nozzle diameter of 0.5 mm fitted on top of syringe holders, as illustrated in Figure 1. PP and PPLP nanocomposite membranes were fabricated by co- electrospinning of the polymer solutions at flow rate (0.5 $mL.h^{-1}$) and speed of drum (30 rpm), DC voltage (19 kV), and 10 cm tip distance. The aluminum covered collecting drum was used for collecting the prepared membranes. The collected membranes were subsequently kept for drying for 24 h at ambient temperature. The prepared nanocomposite membranes were peeled off by employing tweezers for subsequent use in adsorption experiments.

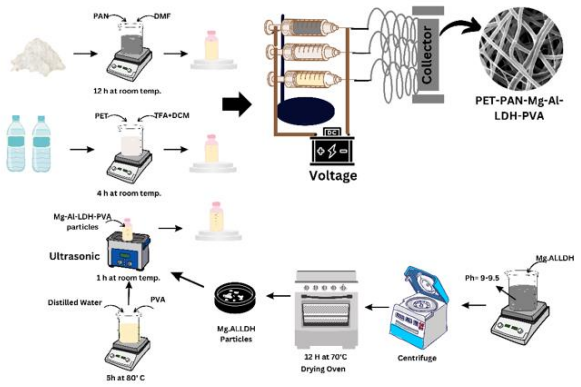

Figure 1. Schematic representation of electrospinning setup for synthesis of PET-PAN-Mg-Al-LDH-PVA nanocomposite membrane

2.5. Characterization techniques

The physico-chemical properties of the membranes were verified with a variety of techniques. Scanning electron microscopy (SEM, JSM-IT-100, JEOL, Tokyo, Japan) analysis was applied for studying the morphology of the as prepared nanocomposite membrane. To find the average fiber diameter of electrospun membrane ImageJ software version 1.54-d was utilized for the measurement of 50 fibers diameter distribution. The phase structure and crystal orientation were identified by using Xray diffraction (XRD, D8 Advance, Bruker, Mannheim, Germany). Energy dispersive Xray spectroscopy (EDS, JSM-IT-100, JEOL, Tokyo, Japan) was utilized to analyze membrane's elemental composition. Likewise, infrared spectroscopic analysis of chemical structure and functional groups of membrane was achieved utilizing Fourier Transform Infrared Spectroscopy (FTIR, Perkin Elmer, Waltham, USA) technique. Hydrophilic behavior of the synthesized membrane was determined by water contact angle test.

2.6. Adsorption experiments of EBT and MB

Developed membranes adsorption properties were assessed through basic experiments and were conducted in a 20 mL volume beaker containing EBT and MB aqueous solutions for each set of experiments. Optimization for the assessment of EBT, several parameters were varied one by one like adsorption time 30 ~ 120 min, pollutant concentration 10 ~ 30 $mg.L^{-1}$, membrane dosage 10 ~ 50 mg and pH 1 ~ 9. A similar method was adopted for the assessment of MB at the optimum parameters, contain pH (7.0), pollutant concentration (10 $mg.L^{-1}$), membrane dosage (30 mg) and adsorption time (120 min). The solutions pH was maintained with the help of 0.01 M HCL and 0.01 M NaOH. The membranes were taken out from the beakers after the completion of the batch experiments. EBT and MB solutions concentration were estimated by means of UV-Vis spectrophotometer (L7 dual beam, BioBase, Jinan, China) at absorbance wavelength of 530 nm and 665 nm, respectively.

The equations (1 and 2) given below were utilized for measuring the percent of adsorption capacity and removal efficiency of EBT and MB (da Silva *et al*. 2021; Mansor *et al.* 2020; Manzar *et al*. 2019).

$$q_{e=}\frac{(C_o - C_f)}{m} x V \quad (1)$$

$$Dye\,Removal(\%) = \frac{(C_o - C_f)}{C_o} x 100 \quad (2)$$

Here "C_0" stands for the pollutant initial concentration of EBT and MB in mg L^{-1}, while "C_f" is the dye final concentration of EBT and MB in mg L^{-1}, respectively. "qe" represents the quantity of EBT and MB adsorbed on the surface of membrane in ($mg.g^{-1}$). While "m" represents weight dosage of the adsorbent in (g), and 'V' denotes the volume in (mL) of pollutant solution.

2.7. Isotherms and kinetic models

2.7.1. Adsorption Isotherms

Adsorption isotherm models i.e. Langmuir and Freundlich were applied to examine the isotherm of adsorption for the pollutants. As depicted in the model (Langmuir isotherm), the optimum adsorption level is determined by the monolayer adsorption. The surface equilibrium point shows the maximum adsorption in Langmuir isotherm model, and it presented in equation 3 as below (Guo *et al*. 2021; Habiba *et al.* 2019).

$$\frac{C_e}{q_e} = \frac{C_e}{q_m} + \frac{1}{K_L q_m} \quad (3)$$

In this, "C_e" indicates the mg L^{-1} of pollutant concentration equilibrium, "q_e" is the mg g^{-1} of adsorption capacity equilibrium. "K_L" represents the solution affinity, whereas "q_m" is the dye maximum adsorption.

The multilayer process of adsorption for a heterogenous system can be defined by the Freundlich isotherm model.

This model can be written as following equation 4 (Pathirana *et al.* 2023).

$$\ln q_e = \ln(k_f) + \ln\frac{C_e}{n} \quad (4)$$

Here, "1/*n*" indicates the adsorption intensity, and "k_f" is a constant value.

2.7.2. Adsorption kinetics

The process of adsorption kinetics can calculate the adsorbent's rate of pollutant adsorption. To know the mechanism of adsorption of the membrane, Pseudo-1st- order and 2nd- order kinetics models were utilized. Pseudo-1st- order kinetic adsorption model applies to physical adsorption process, whereas, chemical adsorption relates to pseudo-2nd- order kinetic model (He *et al*. 2019). The below equations 5 and 6 were used for the kinetic calculations in relation to the pseudo 1st- order and 2nd- order kinetic adsorption models, respectively (Radoor, Karayil, Jayakumar, Parameswaranpillai, & Siengchin 2021).

$$\log(q_e - q_t) = Logq_{-}\frac{k_1}{2.303}t \quad (5)$$

$$\frac{t}{q_t} = \frac{1}{k_2 q_e^2} + \frac{t}{q_e} \quad (6)$$

Whereas "q_t" represents the adsorption capacity in mg/g at time "t", "q_e" is the mg/g of the adsorbate quantity adsorbed at equilibrium. Whereas "k_1" and "k_2" are utilized for the 1st order and 2nd order adsorption rate constant.

3. Results and discussion

3.1. Membrane characterization results

3.1.1. Surface morphology results

The morphology of PP, $PPLP_1$, $PPLP_2$, and $PPLP_3$ membranes surface with different loading of Mg-Al-LDH were investigated by SEM. The morphology image of PP membrane displays the very smooth distribution of nanofibers as shown in Figure 2(a). Similarly, modified nanocomposite membranes $PPLP_1$, $PPLP_2$, and $PPLP_3$ with Mg-Al-LDH-Hybrid revealed the rough and porous structure as compared to the unmodified PP nanomembrane as depicted in Figures 2(b-d), respectively. The synthesized nanoparticles Mg-Al-LDH represent the irregular cubicles and dispersed non uniform porous agglomerates (Abdollahi *et al.* 2021; Alnaqbi *et al*. 2020; Qin *et al*. 2012). The modified membranes fiber diameter $PPLP_1$ (623 nm), $PPLP_2$ (655 nm), and $PPLP_3$(671 nm) were achieved to be greater, as compared to the PP (488 nm) as depicted in supplementary information Figure S1(a-d). The increase in fiber diameter of the modified membrane was due to the modification with LDH hybrid. The major factor that influences the enhancement in nanofiber diameter is solution viscosity. The increase in nanofiber diameter with increase in viscosity is discussed in previous studies (Bakhsh *et al.* 2021; Habiba *et al.* 2017; Nasouri *et al.* 2015; S. Wu *et al.* 2022).

3.1.2. EDS analysis results

The elemental composition of the modified ($PPLP_1$, $PPLP_2$, and $PPLP_3$) and nonmodified (PP) electrospun membranes and Mg-Al-LDH nanoparticles were identified by using the EDS technique, as depicted in Table 1 and supplementary information Figure S2. The nonmodified PP membrane contains only C, N, and O elements. While modified PPLP membranes contain Mg and Al atoms along with C, N, and O elements. According to Table 1, the elements (Mg and Al) atomic % values were higher (0.25 and 0.63) in $PPLP_3$ membrane with increasing LDH loading as compared with other membranes. The EDS spectrum displays the occurrence of elements (Mg, Al, O, C, and N) that confirms the successfully fabrication of modified membrane.

3.1.3. FTIR results

Figure 3(a) represents the functional groups characterization of modified ($PPLP_3$) and unmodified (PP) membranes were analysis by FTIR technique. PAN nanofibers spectra presented the characteristics peaks due to stretching vibration of –CH2– occurred at 1455 cm^{-1} and 1073 cm^{-1}. The stretching bands of nitrile group –C≡N of PAN nanofibers revealed the characteristics peak at 2280 cm^{-1} (Hartati *et al*. 2022; Shakiba *et al.* 2023; Xu *et al*. 2022). The PET peaks were occurred at 2910 cm^{-1} and 1770 cm^{-1} representing to be formed by methylene groups (-CH2-) longitudinal and oscillation of carbonyl (C = O) group, respectively (Khorram *et al*. 2017). The PVA spectrum, resonance band were appeared at 3395 cm^{-1} due to the presence of the –OH group and characteristics band of C-H group was observed at 2909 cm^{-1} (S. Wu *et al*. 2022). The developed Mg-Al-LDH nanoparticles spectrum band at 3395 cm^{-1}, were due to the existence of hydroxyl (OH) vibration stretching. Peaks at 1355 cm^{-1} and 1670 cm^{-1} occurred by the presence of NO_3^- (Novillo *et al*. 2014). The characteristics bands confirm the fabrication of modified and unmodified membranes.

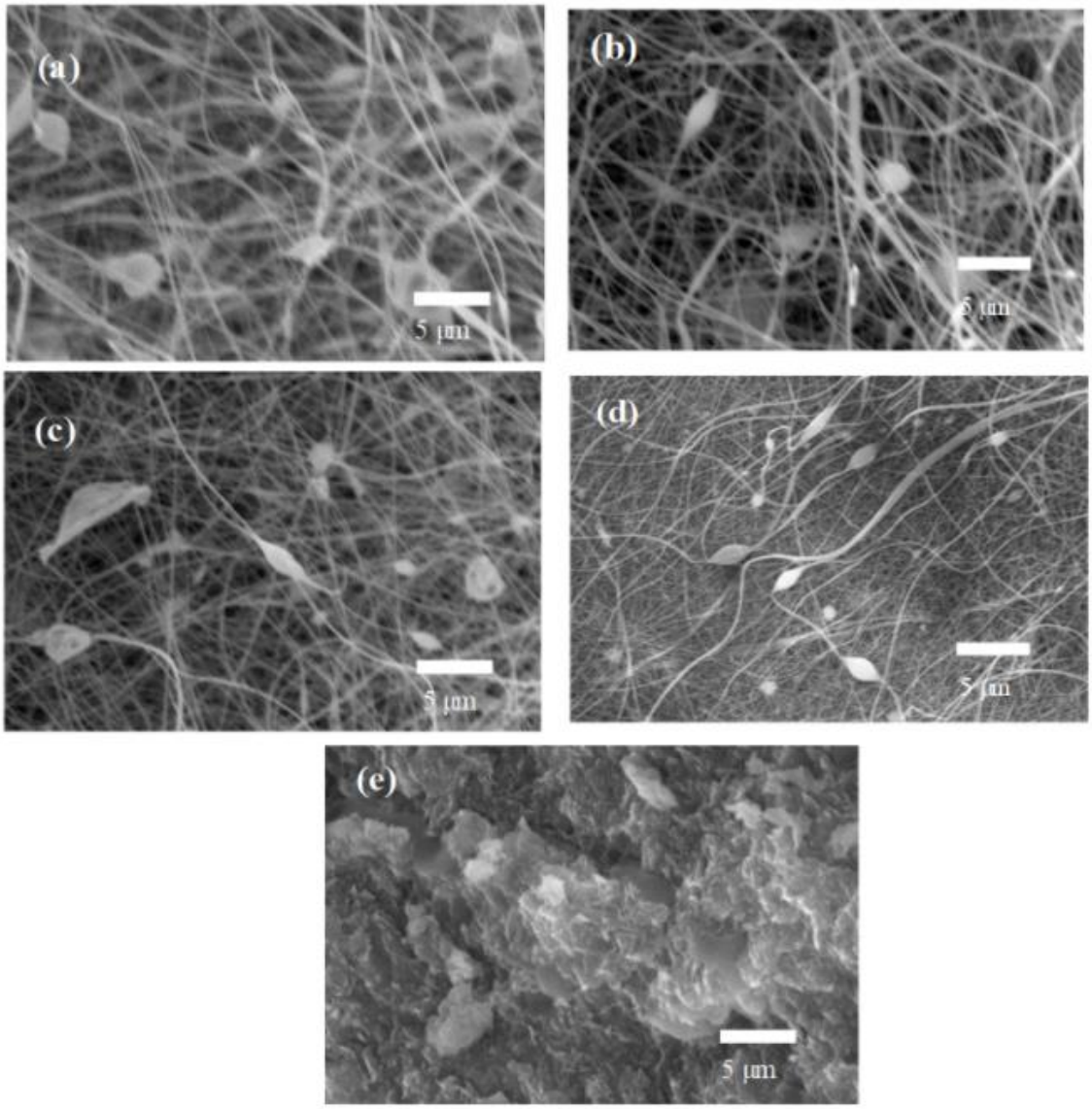

Figure 2. The surface morphology images of: (a) PP, (b) PPLP1, (c) PPLP2, (d) PPLP3 and (e) Mg-Al-LDH nanoparticles

Table 1. EDS elemental composition (atomic %) of PP, $PPLP_1$, $PPLP_2$, $PPLP_3$, and Mg-Al-LDH

Sr #	Type	Mg	Al	C	N	O
1	LDH	15.11	5.30	11.93	-	67.40
2	PP	-	-	89.49	5.14	5.37
3	$PPLP_1$	0.21	0.19	62.46	5..81	31.33
4	$PPLP_2$	0.37	0.24	55..79	5.37	38.23
5	$PPLP_3$	0.63	0.25	60.02	6.45	32.65

3.1.4. XRD results

Figure 3(b) displayed the XRD analysis of PP and $PPLP_3$ membranes. The XRD pattern observed for PET displayed peak at 2θ = 17° (Aziz *et al*. 2021; Q. Wang *et al.* 2015; Yasin *et al.* 2021). Whereas three sharp diffraction peaks of PAN were identified at 2θ = 18°, 22 °, and 26° that represent to the crystalline structure (Chiu *et al.* 2011; Makarov *et al*. 2022; Ullah *et al*. 2019). Furthermore, major sharp peaks of Mg-Al-LDH nanoparticles were occurred at 2θ = 31° and 44^0 (Alnaqbi *et al*. 2020; Swain *et al.* 2018). The XRD pattern for PVA was observed at peak 2θ = 19.5° (Qin *et al*. 2012). The result of XRD analysis of PET, PAN, LDH and PVA showed the successful synthesis of PPLP membrane.

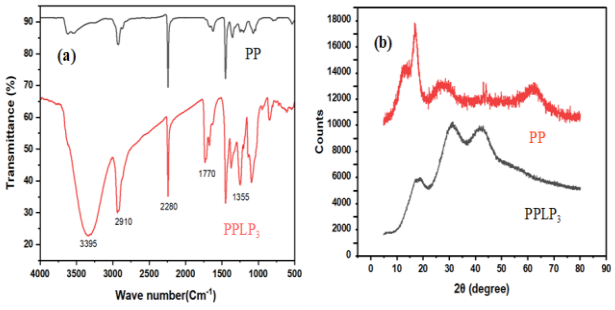

Figure 3. PP and PPLP3 membranes: (a) FTIR spectrum and (b) XRD analysis

3.1.5. Hydrophilicity measurement

The wettability performance of PP and $PPLP_3$ nanocomposite membranes was measured by water contact angle technique. As shown in Figure 4, the water contact angle of $PPLP_3$ membrane (19^o) is lower than the PP membrane (81^o). The reduction in contact angle values of $PPLP_3$ electrospun membrane showed better hydrophilicity properties as compared to the PP membrane. Increased in membrane hydrophilicity may be due to the cause of surface roughness (Jiang *et al.* 2004; X. Li *et al.* 2009; Skornyakov & Komar 1998; N. Wang *et al.* 2008). The wettability of the $PPLP_3$ membrane increased may also be due to the addition of LDH-hybrid (Jia *et al.* 2021; G. Li *et al.* 2013). The decrease in water contact angle will help to enhance the adsorption of pollutant removal from wastewater.

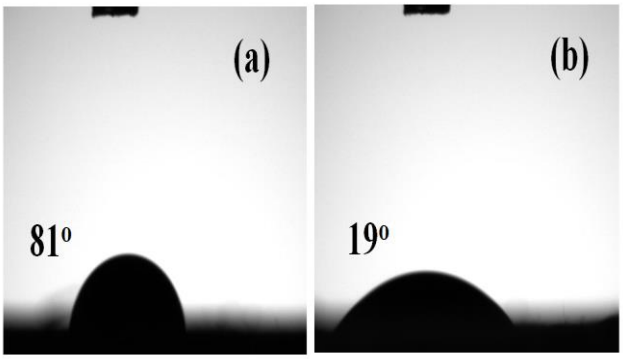

Figure 4. Hydrophilicity analysis using water contact angle test: (a) PP and (b) $PPLP_3$ membranes

3.2. Initial adsorption experiment results

Firstly, basic experiments were achieved to examine the adsorption efficiency of the modified $PPLP_1$, $PPLP_2$, and $PPLP_3$ membranes and nonmodified PP membranes for EBT and MB dyes. $PPLP_3$ membrane removal efficiency for pollutants EBT (83%) and MB (52%) is higher than that of other membranes as shown in supplementary information Figure S3. The increased removal efficiency of pollutants occurred through the surface phenomena, wettability, and the existence of the functional groups on the surface of membrane (C–N, C–O, –OH, etc.). The $PPLP_3$ membrane was used to perform additional experiment trials for kinetic and adsorption isotherm models. The parameters to check the adsorption efficiency of MB and EBT are shown in supplementary information Table S1.

3.3. Optimization of adsorption experiment

3.3.1. pH

A solution's pH significantly affects the adsorption process as it influences both efficiency and behavior of adsorption method. The minor variation in the solution's initial pH could affect the removal efficiency, while it also influencing the solution's properties and the membrane surface charge (Anah & Astrini 2017). The experimental design for the assessment of EBT adsorption on the surface of membrane was performed with the variation in pH 1 ~ 9 keeping initial pollutant concentration (10 $mg.L^{-1}$), adsorption time (90 min), and membrane dose (30 mg). It was observed that at pH 3 the EBT adsorption shows maximum removal efficiency 83% as presented in Figure 5(a). From the experimental results it was identified that when the solution pH was increased, the removal efficiency of EBT decreases. At pH 3, maximum adsorption performance obtained may be associated to the surface characteristics of the electrospun membrane (Radoor *et al*. 2021; Xu *et al*. 2022).

3.3.2. Initial dye concentration

In order to examine impact on the adsorption of EBT, the pollutant concentration was adjusted in between 10 to 30 mg L^{-1}. With the gradual rise in the pollutant concentration, there was a drop in the efficacy of EBT adsorption; Figure 5(b) shows that the optimum removal performance of EBT was at 10 $mg.L^{-1}$. Higher pollutant concentration leads to decrease in percentage of dye elimination at the same adsorption time (Khan *et al*. 2021; Y. Wu *et al*. 2013).

3.3.3. Contact time

Several tests were carried out to obtain maximum equilibrium time that tends to offer the optimum EBT adsorption. The adsorption efficiency of EBT at varying contact times (30 ~ 120 min) are shown in Figure 5(c). Because of the existence of adsorption functional groups and active sites on the $PPLP_3$ membrane surface, the adsorption efficiency values for EBT increased initially. Later, a gradual trend was noticed till it achieves equilibrium condition which was attained after 90 min. It has been noted that the active sites on the membrane surface of every polymer has a separate equilibrium duration due to the active functional groups (Chaukura *et al.* 2017; Y. Wu *et al*. 2013).

3.3.4. Membrane dosage

The dosage of the adsorbent is also one of the significant factors that influence the membrane materials adsorption efficiency. Varying in the adsorbent dosage of $PPLP_3$ from 10 ~ 50 mg the efficiency of the removal of EBT was analyzed. It was observed that the increase in the membrane dosage results in an improved pollutant adsorption by the membrane (Bensalah *et al.* 2020). Therefore, the result shows the enhanced adsorption process is due to the increase of active adsorption sites on the $PPLP_3$ membrane surface, which is because of the increase in membrane dosage (Eltaweil *et al.* 2020). As shown in Figure 5(d), the maximum 95.4% of EBT removal was achieved with a $PPLP_3$ dosage of 50 mg. For further experiments the optimum $PPLP_3$ dosage was selected as 30 mg.

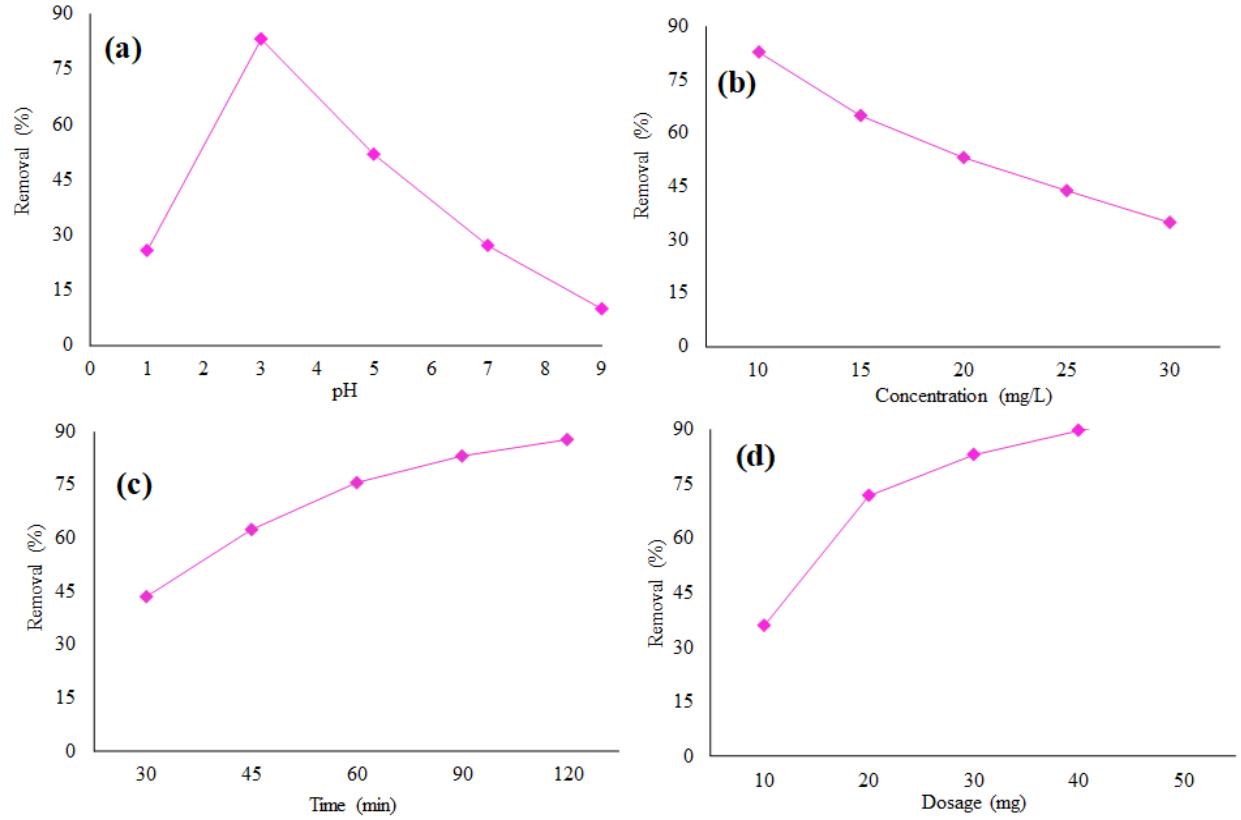

Figure 5. Effect of: (a) solution pH, (b) pollutant concentration, (c) adsorption time, and (d) membrane dosage on EBT removal using PPLP3 membrane

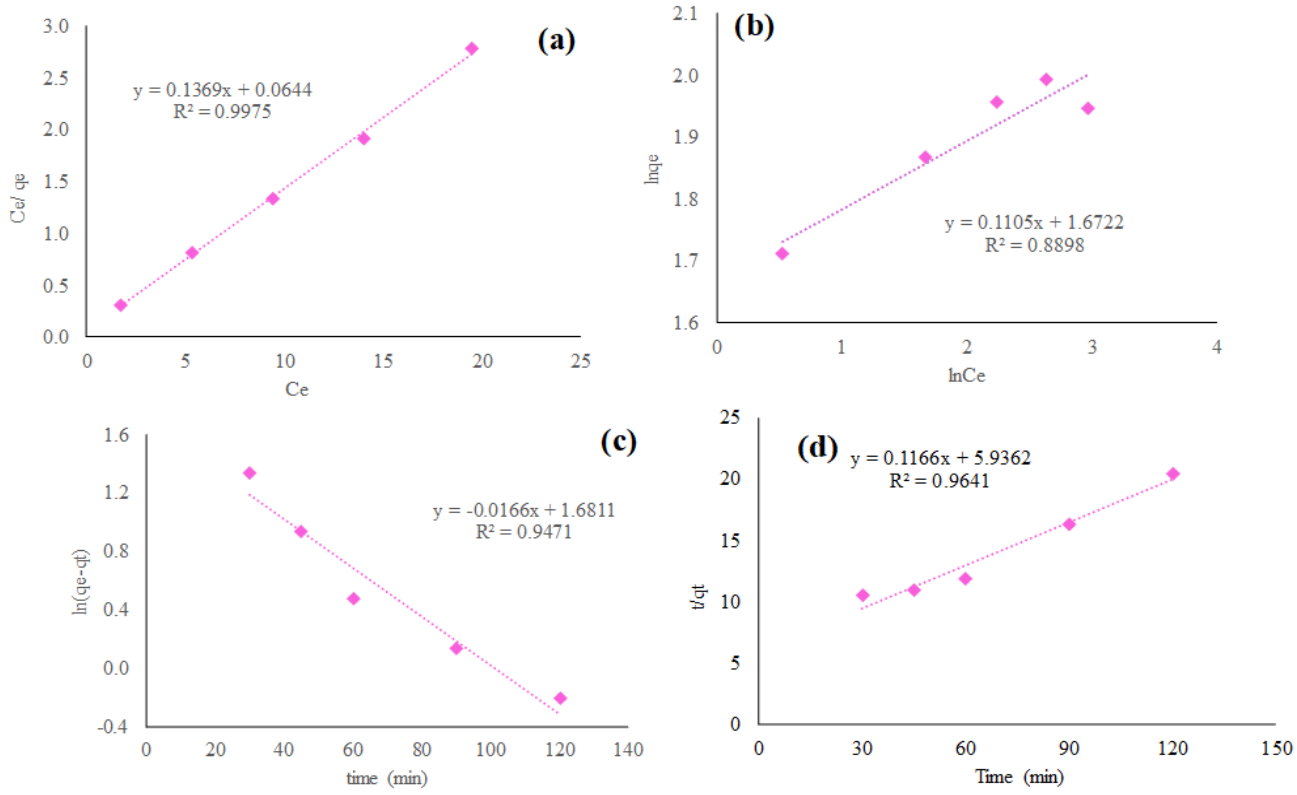

Figure 6. Adsorption isotherm models for EBT: (a) Langmuir and (b) Freundlich. Adsorption kinetic curves of EBT: (c) pseudo-1st order and (d) pseudo-2nd order

3.4. Adsorption Isotherms

The isotherms models i.e. Freundlich and Langmuir were utilized to explore the $PPLP_3$ membrane's adsorption capacity. An adsorption isotherm analysis was achieved to identify the functions of the membrane quantity attached to the membrane's surface (Al-Sou'od 2012). Figure 6(a-b)

and Table 2 present a relationship of the adsorption parameters derived from the Freundlich and Langmuir isotherms model for the adsorption of EBT on $PPLP_3$ nanomembrane surface. For dye adsorption on $PPLP_3$ the Langmuir isotherm was observed suitable with R^2 value of 0.997. According to Table 2, the Langmuir isotherm model was observed to be sufficiently applied to the membrane adsorption process and is suitable to $PPLP_3$ membrane having an optimum EBT adsorption capacity of 7.3 $mg.g^{-1}$.

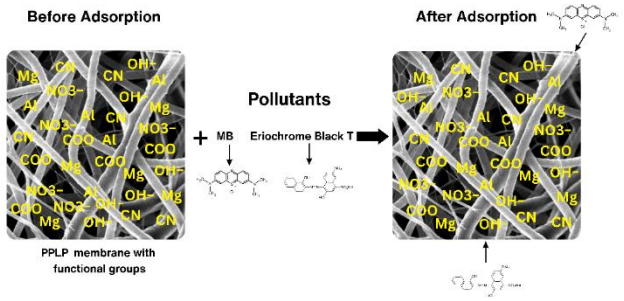

Figure 7. Proposed adsorption mechanism of MB and EBT dyes for PPLP membrane

3.5. Adsorption kinetics

The obtained experimental data were fitted into various kinetic models to examine the adsorption mechanism and adsorption rate constant. As shown in Table 2 and Figure 6(c-d), the pseudo-1st and pseudo-2nd order model parameters were identified, and the corresponding R^2 values were found to be 0.947 and 0.964, respectively. The pseudo-2nd order model gives a well explanation of the EBT adsorption mechanism as compared to the pseudo-1st order model. The pseudo-2nd order model is fit well in the current research, as it is effective at managing the EBT adsorption onto the $PPLP_3$ membrane surface. This also provided that the adsorption mechanism is done through the process of chemisorption process (Konicki *et al.* 2017; L. Li *et al.* 2014).

3.6. Proposed PPLP adsorption mechanism

The adsorption mechanism is primarily caused by ions or liquid molecules adhering on the PPLP membrane surface. It happens because of the reason of force of attraction in between the adsorbent and adsorbate (Konicki *et al*. 2017; L. Li *et al*. 2014). Figure 7 discusses the suggested mechanism process of adsorption in between EBT, MB and the PPLP membrane. It was evident from characterization results that there are different functional groups present in the PPLP membrane. Due to electrostatic force of attraction or hydrogen bond, the dye EBT having N=O functional group is adsorbed on the PPLP membrane (Dhar *et al*. 2022; Zubair *et al*. 2017). Similarly, hydroxyl ions on the PPLP membrane is most likely to participate in MB adsorption through electrostatic force of attraction (Dhar *et al*. 2021; Pan *et al*. 2020). Table 3 displays the comparison performance of $PPLH_3$ membrane with other related studies, which shows that this membrane can remove pollutants efficiently.

Table 2. Parameters for Langmuir and Freundlich adsorption models, pseudo-1st order and pseudo-2nd order kinetic models

Langmuir Isotherm			**Freundlich isotherm**		
q_{max} ($mg\ g^{-1}$)	KL ($L.mg^{-1}$)	R^2	KF ($mg\ g^{-1}$) ($L.mg^{-1}$)1/n	1/n	R^2
7.3	2.126	0.997	5.3	0.1	0.889
Pseudo-1st order			**Pseudo-2nd order**		
q_e ($mg\ g^{-1}$)	k_1 (1/h)	R^2	q_e ($mg\ g^{-1}$)	k_2 ($g.mg^{-1}.h^{-1}$)	R^2
5.37	0.017	0.947	8.58	0.002	0.964

Table 3. Summary of comparative studies of the current research with others related research

Sr No.	Adsorbent type	Target pollutant	Solution pH	Adsorption time (min)	q_{max} ($mg.g^{-1}$)	Reference
1	PET-PAN-Mg-Al-LDH-PVA	EBT	3	90	7.30	This study
2	Polyvinyl Alcohol/Starch/ZSM-5 Zeolite	EBT	3	180	2.17	(Radoor *et al*. 2020)
3	CTAB-PA	EBT	4	--	89.93	(Ben Arfi *et al.* 2019)
4	PET NF-MWCNTs	MB	8	120	7.05	(Essa *et al*. 2022)
5	OMWCNT-K-Carrageenan-Fe_3O_4	MB	--	360	1.24	(Duman *et al.* 2016)

4. Conclusions

The nanocomposite membrane was successfully synthesized using PET-PAN modified with Mg-Al-LDH hybrid with the electrospinning technique, and was confirmed by SEM, EDS, FTIR, and XRD results. From SEM results it was observed that the membrane diameter was increased with addition of LDH hybrid. The addition of different concentration of Mg-Al-LDH, the PPLP membrane's hydrophilicity was improved with notable adsorption efficiency of 83% for EBT and 52% for MB, respectively. Adsorption of MB and EBT on the surface of $PPLP_3$ membrane is pH dependent. The adsorption of PPLP membrane's follows the pseudo-2nd-order kinetics model and the Langmuir isotherm adsorption model, with R^2 values of 0.964 and 0.997, respectively. The adsorption mechanism suggested that the pollutants were removed due to the presence of functional groups on PPLP membrane surface. Results show that $PPLP_3$ has good adsorptive properties for a variety of pollutants from wastewater, therefore, it could be used as a potential adsorbent in the future.

Abbreviation	Details
PET	Polyethylene terephthalate
PAN	Polyacrylonitrile
LDH	Layer double hydroxides
PVA	Polyvinyl alcohol
EBT	Eriochrome Black T
MB	Methylene blue
Mw	Molecular weight
$Mg(NO_3)_2.6H_2O$	Magnesium nitrate hexahydrate
$Al(NO_3)_3.9H_2O$	Aluminum nitrate nonahydrate
Na_2CO_3	Sodium carbonate
HCl	Hydrochloric acid
NaOH	Sodium hydroxide pellets
H_2SO_4	Sulfuric acid
DMF	N, N-Dimethyl formamide
TFA	Trifluoro acetic acid
DCM	Dichloro methane
SEM	Scanning electron microscopy
XRD	Xray diffraction
EDS	Energy dispersive Xray spectroscopy
FTIR	Fourier Transform Infrared Spectroscopy
PP	PET-PAN
PPLP	PET-PAN-Mg-Al-LDH-PVA

Acknowledgments

The authors acknowledge the support by Sindh Madressatul Islam University for giving the experimental research laboratory facilities.

Conflicts of Interest

There are no conflicts of interest to declare.

References

Abdollahi E., Heidari A., Mohammadi T., Asadi A.A. and Tofighy M.A. (2021). Application of Mg-Al LDH nanoparticles to enhance flux, hydrophilicity and antifouling properties of PVDF ultrafiltration membrane: Experimental and modeling studies. *Separation and purification technology,* ***257***, 117931.

Ahmad A., Mohd-Setapar S.H., Chuong C.S., Khatoon A., Wani W.A., Kumar R. and Rafatullah M. (2015). Recent advances in new generation dye removal technologies: novel search for approaches to reprocess wastewater. *RSC advances,* ***5***(39), 30801–30818.

Akram M., Bhutto S.U.A., Aftab S., Sindhu L., Xu X. and Haider Z. (2023). Nanocomposites for Removal and Degradation of Organic Pollutants. In *Modern Nanotechnology: Volume 1: Environmental Sustainability and Remediation* (pp. 519–558): Springer.

Al-Sou'od K. (2012). Adsorption isotherm studies of chromium (VI) from aqueous solutions using Jordanian pottery materials. *Apcbee Procedia,* ***1***, 116–125.

Aldawsari A.M., Alsohaimi I., Hassan H.M., Abdalla Z.E., Hassan I. and Berber M.R. (2021). Tailoring an efficient nanocomposite of activated carbon-layered double hydroxide for elimination of water-soluble dyes. *Journal of Alloys and Compounds,* ***857***, 157551.

Alnaqbi M.A., Samson J.A. and Greish Y.E. (2020). Electrospun polystyrene/LDH fibrous membranes for the removal of Cd2+ ions. *Journal of Nanomaterials, 2020*, 1–12.

Anah L. and Astrini N. (2017). *Influence of pH on Cr (VI) ions removal from aqueous solutions using carboxymethyl cellulose-based hydrogel as adsorbent.* Paper presented at the IOP Conference Series: Earth and Environmental Science.

Anandh Babu M., Hemavathi S., Kousalyadevi G. and Shanmuga Priya S. (2023). Biosorption potential of neem leave powder for the sequestration of arsenic and chromium metal ions.

Ayandiran T., Fawole O. and Dahunsi S. (2018). Water quality assessment of bitumen polluted Oluwa river, South-Western Nigeria. *Water Resources and Industry,* ***19***, 13–24.

Aziz F.M.A., Surip S.N., Sekak K.A., Uyup M. K.A., Tarawneh M.a.A. and Lee S.H. (2021). Evaluation of wetting, structural and thermal properties of electrospun nanofibers at different pineapple leaf fiber/polyethylene terephthalate ratios. *Maderas. Ciencia y tecnología,* ***23***.

Baig N., Matin A., Faizan M., Anand D., Ahmad I. and Khan S.A. (2022). Antifouling low-pressure highly permeable single step produced loose nanofiltration polysulfone membrane for efficient Erichrome Black T/divalent salts fractionation. *Journal of Environmental Chemical Engineering,* ***10***(4), 108166.

Bakhsh N., Ahmed Z., Mahar R.B. and Khatri Z. (2021). Development and application of electrospun modified polyvinylidene fluoride (PVDF) nanofibers membrane for biofouling control in membrane bioreactor. *Desalin. Water Treat*, 74–82.

Bano Z., Akram M., Ali N.Z., Khan M.U., Wang F., Li L. and Xia M. (2024). Sustainable porous graphene/Co-MOF for the removal of water pollutants: Combined theoretical and experimental studies. *Journal of Water Process Engineering,* ***59***, 104982.

Ben Arfi R., Karoui S., Mougin K. and Ghorbal A. (2019). Cetyltrimethylammonium bromide-treated Phragmites australis powder as novel polymeric adsorbent for hazardous Eriochrome Black T removal from aqueous solutions. *Polymer bulletin,* ***76***(10), 5077–5102.

Bensalah H., Younssi S.A., Ouammou M., Gurlo A. and Bekheet M.F. (2020). Azo dye adsorption on an industrial waste-transformed hydroxyapatite adsorbent: Kinetics, isotherms, mechanism and regeneration studies. *Journal of Environmental Chemical Engineering,* ***8***(3), 103807.

Chaukura N., Murimba E.C. and Gwenzi W. (2017). Synthesis, characterisation and methyl orange adsorption capacity of ferric oxide–biochar nano-composites derived from pulp and paper sludge. *Applied Water Science,* ***7***, 2175–2186.

Cheng J., Zhan C., Wu J., Cui Z., Si J., Wang Q. and Turng L.-S. (2020). Highly efficient removal of methylene blue dye from an aqueous solution using cellulose acetate nanofibrous membranes modified by polydopamine. *ACS omega,* ***5***(10), 5389–5400.

Chiu H., Lin J., Cheng T. and Chou S. (2011). Fabrication of electrospun polyacrylonitrile ion-exchange membranes for application in lysozym. *Express Polymer Letters,* ***5***(4).

da Silva Alves D.C., Healy B., Pinto L.A.d.A., Cadaval Jr T.R.S.A. and Breslin C.B. (2021). Recent developments in chitosan-based adsorbents for the removal of pollutants from aqueous environments. *Molecules,* ***26***(3), 594.

da Silva R.J., Mojica-Sánchez L.C., Gorza F.D., Pedro G.C., Maciel B.G., Ratkovski G.P. and Chávez-Guajardo A.E. (2021). Kinetics and thermodynamic studies of Methyl Orange removal by polyvinylidene fluoride-PEDOT mats. *Journal of Environmental Sciences,* ***100***, 62–73.

Dai S., Wu X., Zhang J., Fu Y. and Li W. (2018). Coenzyme A-regulated Pd nanocatalysts for formic acid-mediated reduction of hexavalent chromium. *Chemical Engineering Journal,* ***351***, 959–966.

Dhar L., Hossain S., Rahman M.S., Quraishi S. B., Saha, K., Rahman, F., & Rahman, M. T. (2021). Adsorption mechanism of methylene blue by graphene oxide-shielded Mg–Al-layered double hydroxide from synthetic wastewater. *The Journal of Physical Chemistry A,* ***125***(4), 954–965.

Dhar L., Rahman M.S., Hossain S., Quraishi S.B., Saha K., Rahman F. and Rahman M.T. (2022). Mechanistic insights of the adsorption of Eriochrome Black T by the formulated Mg–Al LDH-graphene oxide composite. *Journal of the Iranian Chemical Society,* ***19***(4), 1319–1328.

Duman O., Tunç S., Polat, T.G. and Bozoğlan B.K. (2016). Synthesis of magnetic oxidized multiwalled carbon nanotube-κ-carrageenan-Fe3O4 nanocomposite adsorbent and its application in cationic Methylene Blue dye adsorption. *Carbohydrate Polymers,* **147**, 79–88.

Ebrahimi F., Nabavi S.R. and Omrani A. (2022). Fabrication of hydrophilic hierarchical PAN/SiO2 nanofibers by electrospray assisted electrospinning for efficient removal of cationic dyes. *Environmental Technology & Innovation,* ***25***, 102258.

Eltaweil A., Mohamed H.A., Abd El-Monaem E.M. and El-Subruiti G. (2020). Mesoporous magnetic biochar composite for enhanced adsorption of malachite green dye: Characterization, adsorption kinetics, thermodynamics and isotherms. *Advanced Powder Technology,* ***31***(3), 1253–1263.

Essa W.K., Yasin S.A., Abdullah A.H., Thalji M.R., Saeed I.A., Assiri M.A. and Ali G.A. (2022). Taguchi L25 (54) Approach for Methylene Blue Removal by Polyethylene Terephthalate Nanofiber-Multi-Walled Carbon Nanotube Composite. *Water,* ***14***(8), 1242.

Farooqi Z.H., Akram M.W., Begum R., Wu W. and Irfan A. (2021). Inorganic nanoparticles for reduction of hexavalent chromium: Physicochemical aspects. *Journal of hazardous materials,* ***402***, 123535.

Guo R., Guo W., Pei H., Wang B., Guo X., Liu N. and Mo Z. (2021). Polypyrrole deposited electrospun PAN/PEI nanofiber membrane designed for high efficient adsorption of chromium ions (VI) in aqueous solution. *Colloids and Surfaces A: Physicochemical and Engineering Aspects,* ***627***, 127183.

Habiba U., Afifi A.M., Salleh A. and Ang B.C. (2017). Chitosan/(polyvinyl alcohol)/zeolite electrospun composite nanofibrous membrane for adsorption of Cr6+, Fe3+ and Ni2+. *Journal of hazardous materials,* ***322***, 182–194.

Habiba U., Lee J.J.L., Joo T.C., Ang B.C. and Afifi A.M. (2019). Degradation of methyl orange and congo red by using chitosan/polyvinyl alcohol/TiO2 electrospun nanofibrous membrane. *International Journal of Biological Macromolecules,* ***131***, 821–827.

Hartati S., Zulfi A., Maulida P.Y.D., Yudhowijoyo A., Dioktyanto M., Saputro K.E. and Rochman N.T. (2022). Synthesis of electrospun PAN/TiO2/Ag nanofibers membrane as potential air filtration media with photocatalytic activity. *ACS omega, 7*(12), 10516–10525.

He Y., Wu P., Xiao W., Li G., Yi J., He Y. and Duan Y. (2019). Efficient removal of Pb (II) from aqueous solution by a novel ion imprinted magnetic biosorbent: Adsorption kinetics and mechanisms. *PloS one,* ***14***(3), e0213377.

Hu W., Wu X., Jiao F., Yang W. and Zhou Y. (2016). Preparation and characterization of magnetic Fe3O4@ sulfonated β-cyclodextrin intercalated layered double hydroxides for methylene blue removal. *Desalination and Water Treatment,* ***57***(53), 25830–25841.

Hu Z.-P., Gao Z.-M., Liu X. and Yuan Z.-Y. (2018). High-surface-area activated red mud for efficient removal of methylene blue from wastewater. *Adsorption Science & Technology,* ***36***(1-2), 62–79.

Inam M.A., Khan R., Lee K.H., Akram M., Ahmed Z., Lee K.G. and Wie Y.M. (2021). Adsorption capacities of iron hydroxide for arsenate and arsenite removal from water by chemical coagulation: Kinetics, thermodynamics and equilibrium Studies. *Molecules,* ***26***(22), 7046.

Jeong C.-B., Lee Y.H., Park J.C., Kang H.-M., Hagiwara A. and Lee J.-S. (2019). Effects of metal-polluted seawater on life parameters and the induction of oxidative stress in the marine rotifer Brachionus koreanus. *Comparative Biochemistry and Physiology Part C: Toxicology & Pharmacology,* ***225***, 108576.

Jia S., Liang Y. and Yang N. (2021). High performance of polyacrylonitrile/[MgAl]-layered double hydroxide composite nanofiber separators for safe lithium-ion batteries. *Solid State Ionics,* ***370***, 115735.

Jiang L., Zhao Y. and Zhai J. (2004). A lotus-leaf-like superhydrophobic surface: a porous microsphere/nanofiber composite film prepared by electrohydrodynamics. *Angewandte Chemie-International Edition,* ***43***(33), 4338–4341.

Khalid A., Zubair M. and Ihsanullah. (2018). A comparative study on the adsorption of Eriochrome Black T dye from aqueous solution on graphene and acid-modified graphene. *Arabian Journal for Science and Engineering,* ***43***, 2167–2179.

Khan M.I., Shanableh A., Fernandez J., Lashari M.H., Shahida S., Manzoor S. and Elboughdiri N. (2021). Synthesis of dmea-

grafted anion exchange membrane for adsorptive discharge of methyl orange from wastewaters. *Membranes,* **11**(3), 166.

Khorram M., Mousavi A. and Mehranbod N. (2017). Chromium removal using adsorptive membranes composed of electrospun plasma-treated functionalized polyethylene terephthalate (PET) with chitosan. *Journal of Environmental Chemical Engineering,* ***5***(3), 2366–2377.

Kishore K., Hsu C.-Y., Sridhara S., Odongo J.O., Akram M., Malik J. A. and Manzoor J. (2023). Fundamentals of Nanotechnology for Environmental Engineering. In *Modern Nanotechnology: Volume 1: Environmental Sustainability and Remediation* (pp. 1–19): Springer.

Konicki W., Aleksandrzak M., Moszyński D. and Mijowska E. (2017). Adsorption of anionic azo-dyes from aqueous solutions onto graphene oxide: equilibrium, kinetic and thermodynamic studies. *Journal of colloid and interface science,* **496**, 188–200.

Li G., Zhao Y., Lv M., Shi Y. and Cao D. (2013). Super hydrophilic poly (ethylene terephthalate) (PET)/poly (vinyl alcohol) (PVA) composite fibrous mats with improved mechanical properties prepared via electrospinning process. *Colloids and Surfaces A: Physicochemical and Engineering Aspects,* ***436***, 417–424.

Li L., Luo C., Li X., Duan H. and Wang X. (2014). Preparation of magnetic ionic liquid/chitosan/graphene oxide composite and application for water treatment. *International Journal of Biological Macromolecules,* ***66***, 172–178.

Li X., Ding B., Lin J., Yu J. and Sun G. (2009). Enhanced mechanical properties of superhydrophobic microfibrous polystyrene mats via polyamide 6 nanofibers. *The Journal of Physical Chemistry C,* ***113***(47), 20452–20457.

Makarov I.S., Vinogradov M.I., Golova L.K., Arkharova N.A., Shambilova G.K., Makhatova V.E. and Naukenov M.Z. (2022). Design and Fabrication of Membranes Based on PAN Copolymer Obtained from Solutions in N-methylmorpholine-N-oxide. *Polymers,* ***14***(14), 2861.

Mansor E.S., Ali H. and Abdel-Karim A. (2020). Efficient and reusable polyethylene oxide/polyaniline composite membrane for dye adsorption and filtration. *Colloid and Interface Science Communications,* **39**, 100314.

Manzar M.S., Waheed A., Qazi I.W., Blaisi N.I. and Ullah N. (2019). Synthesis of a novel epibromohydrin modified crosslinked polyamine resin for highly efficient removal of methyl orange and eriochrome black T. *Journal of the Taiwan Institute of Chemical Engineers,* **97**, 424–432.

Mittal J. (2021). Recent progress in the synthesis of Layered Double Hydroxides and their application for the adsorptive removal of dyes: A review. *Journal of Environmental Management,* **295**, 113017.

Nasouri K., Shoushtari A.M. and Mojtahedi M.R.M. (2015). Effects of polymer/solvent systems on electrospun polyvinylpyrrolidone nanofiber morphology and diameter. *Polymer Science Series A,* **57**, 747–755.

Novillo C., Guaya D., Avendaño A.A.-P., Armijos C., Cortina J. and Cota I. (2014). Evaluation of phosphate removal capacity of Mg/Al layered double hydroxides from aqueous solutions. *Fuel,* ***138***, 72–79.

Pan X., Zhang M., Liu H., Ouyang S., Ding N. and Zhang P. (2020). Adsorption behavior and mechanism of acid orange 7 and methylene blue on self-assembled three-dimensional MgAl layered double hydroxide: Experimental and DFT investigation. *Applied Surface Science,* ***522***, 146370.

Pathirana M.A., Dissanayake N.S., Wanasekara N.D., Mahltig B. and Nandasiri G.K. (2023). Chitosan-graphene oxide dip-coated polyacrylonitrile-ethylenediamine electrospun nanofiber membrane for removal of the dye stuffs methylene blue and congo red. *Nanomaterials,* ***13***(3), 498.

Picón D., Vergara-Rubio A., Estevez-Areco S., Cerveny S. and Goyanes S. (2022). Adsorption of Methylene Blue and Tetracycline by Zeolites Immobilized on a PBAT Electrospun Membrane. *Molecules,* ***28***(1), 81.

Pirzada A.M., Ali I., Mallah N.B. and Maitlo G. (2023). Development of Novel PET-PAN Electrospun Nanocomposite Membrane Embedded with Layered Double Hydroxides Hybrid for Efficient Wastewater Treatment. *Polymers,* ***15***(22), 4388.

Preethi G. and Jeyanthi J. (2023). Biosorption of heavy metals using Gracilaria edulis seaweed–batch adsorption, kinetics and thermodynamic studies.

Qin Q., Liu Y., Chen S.C., Zhai F.Y., Jing X.K. and Wang Y.Z. (2012). Electrospinning fabrication and characterization of poly (vinyl alcohol)/layered double hydroxides composite fibers. *Journal of applied polymer science,* ***126***(5), 1556–1563.

Radoor S., Karayil J., Jayakumar A., Parameswaranpillai J. and Siengchin S. (2021). Efficient removal of methyl orange from aqueous solution using mesoporous ZSM-5 zeolite: Synthesis, kinetics and isotherm studies. *Colloids and Surfaces A: Physicochemical and Engineering Aspects,* ***611***, 125852.

Radoor S., Karayil J., Parameswaranpillai J. and Siengchin S. (2020). Adsorption study of anionic dye, Eriochrome black T from aqueous medium using polyvinyl alcohol/starch/ZSM-5 zeolite membrane. *Journal of Polymers and the Environment,* ***28***, 2631–2643.

Sajid M., Jillani S.M.S., Baig N. and Alhooshani K. (2022). Layered double hydroxide-modified membranes for water treatment: Recent advances and prospects. *Chemosphere,* ***287***, 132140.

Shahverdi F., Barati A. and Bayat M. (2022). Effective Methylene Blue Removal from Aqueous Solutions using PVA/Chitosan Electrospun Nanofiber Modified with CeAlO3 Nanoparticles. *Journal of Water and Environmental Nanotechnology,* **7**(1), 55–68.

Shakiba M., Abdouss M., Mazinani S. and Kalaee M.R. (2023). Super-hydrophilic electrospun PAN nanofibrous membrane modified with alkaline treatment and ultrasonic-assisted PANI in-situ polymerization for highly efficient gravity-driven oil/water separation. *Separation and purification technology,* ***309***, 123032.

Skornyakov I. and Komar V. (1998). IR spectra and the structure of plasticized cellulose acetate films. *Journal of applied spectroscopy,* ***65***, 911–918.

Swain S.K., Barik S., Pradhan G.C. and Behera L. (2018). Delamination of Mg-Al layered double hydroxide on starch: change in structural and thermal properties. *Polymer-Plastics Technology and Engineering,* ***57***(15), 1585–1591.

Ullah S., Hashmi M., Kharaghani D., Khan M.Q., Saito Y., Yamamoto T. and Kim I.S. (2019). Antibacterial properties of in situ and surface functionalized impregnation of silver sulfadiazine in polyacrylonitrile nanofiber mats. *International journal of nanomedicine*, 2693–2703.

Wang N., Zhao Y. and Jiang L. (2008). Low-cost, thermoresponsive wettability of surfaces: Poly (N-isopropylacrylamide)/Polystyrene composite films prepared by electrospinning. *Macromolecular Rapid Communications,* ***29***(6), 485–489.

Wang Q., Geng Y., Lu X. and Zhang S. (2015). First-row transition metal-containing ionic liquids as highly active catalysts for the glycolysis of poly (ethylene terephthalate) (PET). *ACS Sustainable Chemistry & Engineering,* ***3***(2), 340–348.

Wu S., Li K., Shi W. and Cai J. (2022). Preparation and performance evaluation of chitosan/polyvinylpyrrolidone/polyvinyl alcohol electrospun nanofiber membrane for heavy metal ions and organic pollutants removal. *International Journal of Biological Macromolecules,* ***210***, 76–84.

Wu Y., Luo H., Wang H., Wang C., Zhang J. and Zhang Z. (2013). Adsorption of hexavalent chromium from aqueous solutions by graphene modified with cetyltrimethylammonium bromide. *Journal of colloid and interface science,* ***394***, 183–191.

Xu P., Wang Y., Wang S., Dai W., Chen N. and Li Q. (2022). Preparation of polyethyleneimine-modified porous polyacrylonitrile electrospun nanofibers for efficient removal of methyl orange. *Journal of Macromolecular Science, Part A,* ***59***(7), 504–512.

Yasin S.A., Sharaf Zeebaree S.Y., Sharaf Zeebaree A.Y., Haji Zebari O.I. and Saeed I.A. (2021). The efficient removal of methylene blue dye using CuO/PET nanocomposite in aqueous solutions. *Catalysts,* ***11***(2), 241.

Zhang Y., Wu B., Xu H., Liu H., Wang M., He Y. and Pan B. (2016). Nanomaterials-enabled water and wastewater treatment. *NanoImpact,* ***3***, 22–39.

Zhao R., Li X., Li Y., Li Y., Sun B., Zhang N. and Wang C. (2017). Functionalized magnetic iron oxide/polyacrylonitrile composite electrospun fibers as effective chromium (VI) adsorbents for water purification. *Journal of colloid and interface science,* ***505***, 1018–1030.

Zhu F., Zheng Y.-M., Zhang B.-G. and Dai Y.-R. (2021). A critical review on the electrospun nanofibrous membranes for the adsorption of heavy metals in water treatment. *Journal of hazardous materials,* ***401***, 123608.

Zubair M., Jarrah N., Manzar M.S., Al-Harthi M., Daud M., Mu'azu N.D. and Haladu S.A. (2017). Adsorption of eriochrome black T from aqueous phase on MgAl-, CoAl-and NiFe-calcined layered double hydroxides: Kinetic, equilibrium and thermodynamic studies. *Journal of Molecular Liquids,* ***230***, 344–352.

Supplementary information

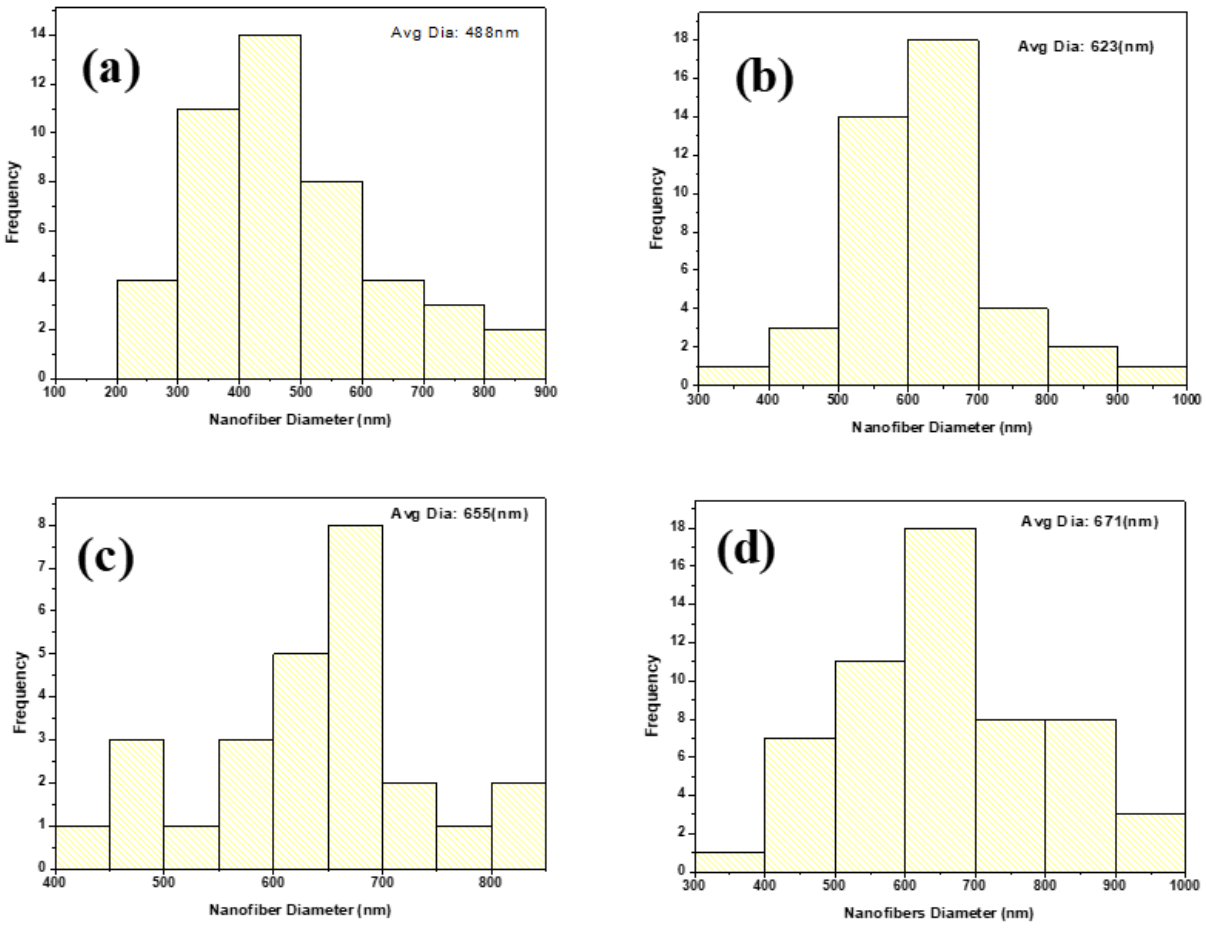

Figure S1. The nanofiber diameter histograms of: (a) PP, (b) PPLP1, (c) PPLP2, and (d) PPLP3 membranes

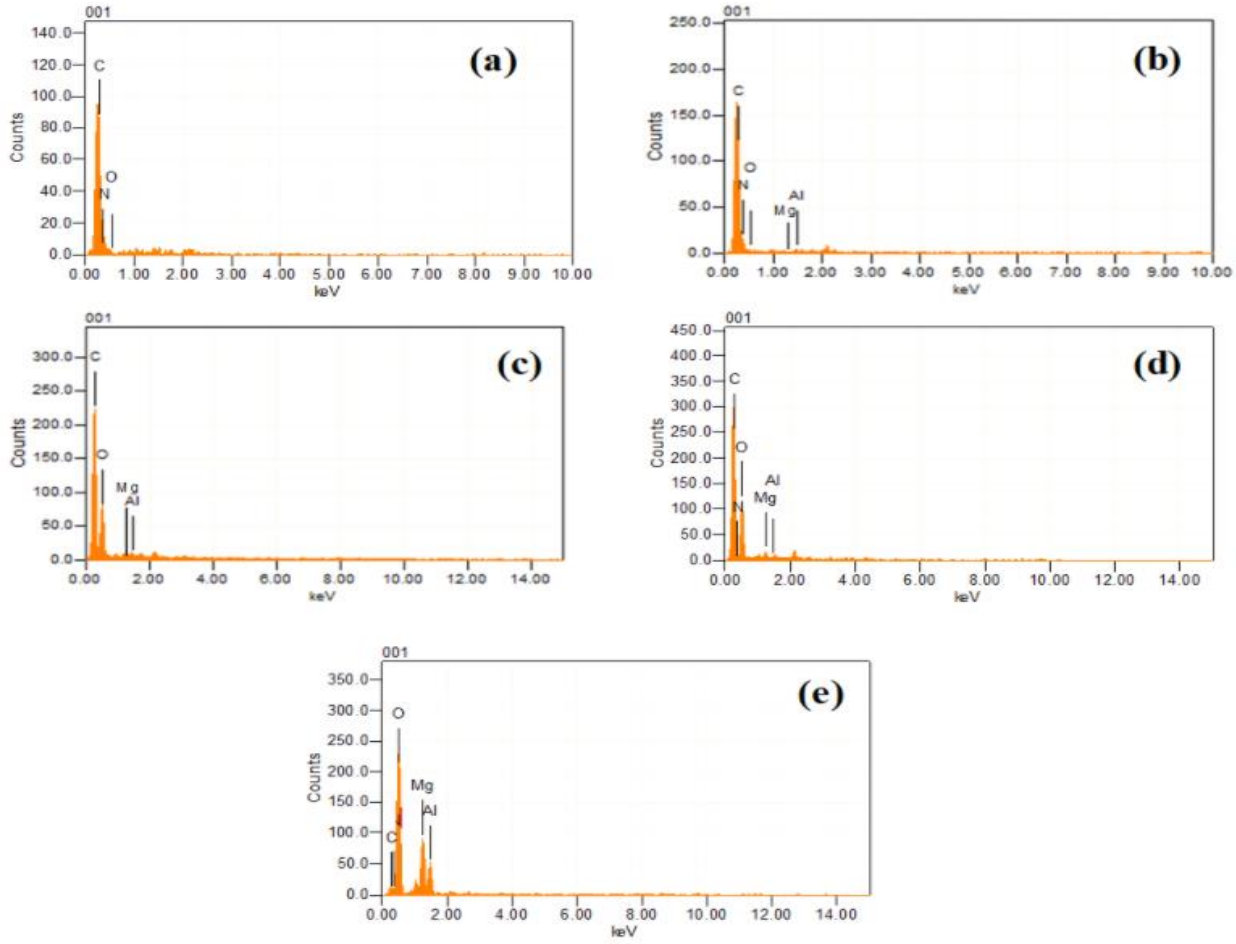

Figure S2. EDS spectrum of: (a) PP, (b) PPLP1, (c) PPLP2, (d) PPLP3, and (e) Mg-Al-LDH

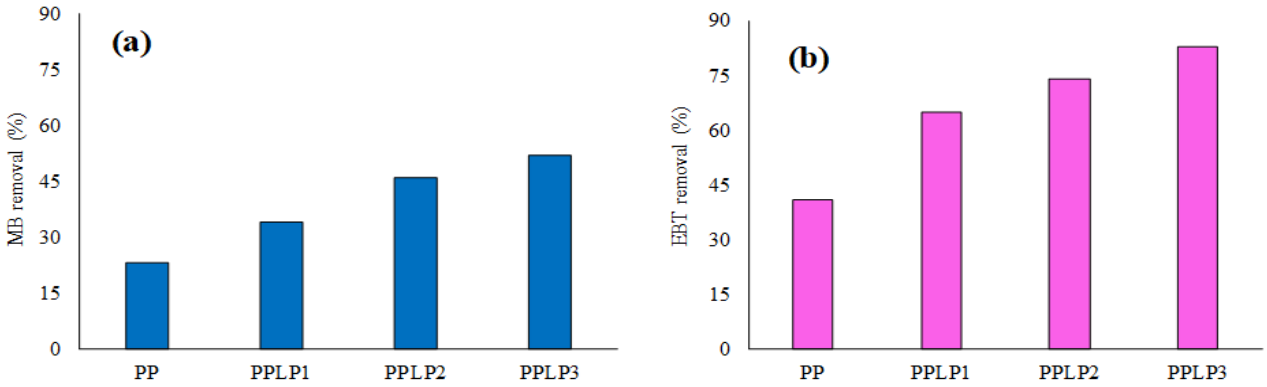

Figure S3. Basic adsorption experiment results for removal of: (a) MB and (b) EBT dyes

Table S1. Basic adsorption experimental conditions for MB and EBT using PP and PPLP membranes

Membrane type	Pollutant type	Solution pH	Adsorption time (min)	Concentration (mg. L^{-1})	Membrane dosage (mg)	Solution volume (mL)
PP	MB	7	120	10	30	20
$PPLP_1$						
$PPLP_2$						
$PPLP_3$						
PP	EBT	3	90	10	30	20
$PPLP_1$						
$PPLP_2$						
$PPLP_3$						